NANO LETTERS

Letter

pubs.acs.org/NanoLett

Electrical Spin Injection and Detection in $Mn_5Ge_3/Ge/Mn_5Ge_3$ Nanowire Transistors

Jianshi Tang,[†,∥] Chiu-Yen Wang,[†,‡,⊥,∥] Li-Te Chang,[†] Yabin Fan,[†] Tianxiao Nie,[†] Michael Chan,[†] Wanjun Jiang,[†] Yu-Ting Chen,[‡] Hong-Jie Yang,[§] Hsing-Yu Tuan,[§] Lih-Juann Chen,*[,‡] and Kang L. Wang*[,†]

[†]Device Research Laboratory, Department of Electrical Engineering, University of California, Los Angeles, California, 90095, United States

[‡]Department of Materials Science and Engineering and [§]Department of Chemical Engineering, National Tsing Hua University, Hsinchu, Taiwan, 30013, Republic of China

[⊥]Department of Materials Science and Engineering, National Taiwan University of Science and Technology, Taipei, Taiwan, 10607, Republic of China

Supporting Information

ABSTRACT: In this Letter, we report the electrical spin injection and detection in Ge nanowire transistors with single-crystalline ferromagnetic Mn_5Ge_3 as source/drain contacts formed by thermal reactions. Degenerate indium dopants were successfully incorporated into as-grown Ge nanowires as p-type doping to alleviate the conductivity mismatch between Ge and Mn_5Ge_3. The magnetoresistance (MR) of the $Mn_5Ge_3/Ge/Mn_5Ge_3$ nanowire transistor was found to be largely affected by the applied bias. Specifically, negative and hysteretic MR curves were observed under a large current bias in the temperature range from T = 2 K up to T = 50 K, which clearly indicated the electrical spin injection from ferromagnetic Mn_5Ge_3 contacts into Ge nanowires. In addition to the bias effect, the MR amplitude was found to exponentially decay with the Ge nanowire channel length; this fact was explained by the dominated Elliot-Yafet spin-relaxation mechanism. The fitting of MR further revealed a spin diffusion length of $l_{sf} = 480 \pm 13$ nm and a spin lifetime exceeding 244 ps at T = 10 K in p-type Ge nanowires, and they showed a weak temperature dependence between 2 and 50 K. Ge nanowires showed a significant enhancement in the measured spin diffusion length and spin lifetime compared with those reported for bulk p-type Ge. Our study of the spin transport in the $Mn_5Ge_3/Ge/Mn_5Ge_3$ nanowire transistor points to a possible realization of spin-based transistors; it may also open up new opportunities to create novel Ge nanowire-based spintronic devices. Furthermore, the simple fabrication process promises a compatible integration into standard Si technology in the future.

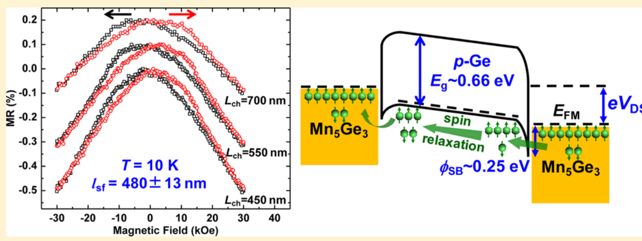

KEYWORDS: *Spin injection and detection, Ge nanowire transistor, Mn_5Ge_3, spin transport, spinFET*

As the aggressive scaling of the physical feature size continues in the complementary metal-oxide-semiconductor (CMOS) technology, there is an urgent need to resolve a number of challenging issues. Among them, the increase in functionality, the decrease in power dissipation, and the reduction in manufacturing variability are of key challenges as highlighted in the *International Technology Roadmap of Semiconductors* (ITRS).[1] Spin-based electronics (spintronics) have emerged as a promising solution in utilizing the spin of electrons as a new degree of freedom for information processing, enabling the creation of novel electronic devices with low power consumption and nonvolatility.[2,3] In the building of semiconductor-based spintronic devices, such as spin field-effect transistor (spinFET) and spin light-emitting diode (spinLED),[3−5] one of the key issues is to realize an efficient spin injection from a ferromagnet (FM) into a semiconductor (SC). Electrical spin injection into various semiconductors, including Si,[6,7] Ge,[8,9] GaAs,[10,11] and graphene,[12,13] has attracted numerous research efforts in the past two decades. While the electrical spin injection into ordinary metals can be easily demonstrated in metallic spin valve structures,[14,15] the realization of efficient spin injection into semiconductors is much complicated by several factors: (1) the huge difference in the conductivity between ordinary ferromagnetic metals and semiconductors would almost make the spin injection efficiency negligibly small, well known as the conductivity mismatch problem;[16] (2) the increase in the doping concentration in order to reduce such a conductivity difference, however, would decrease the carrier spin lifetime due to the aggravated spin relaxation originating from impurity

Received: April 6, 2013
Revised: August 7, 2013
Published: August 12, 2013

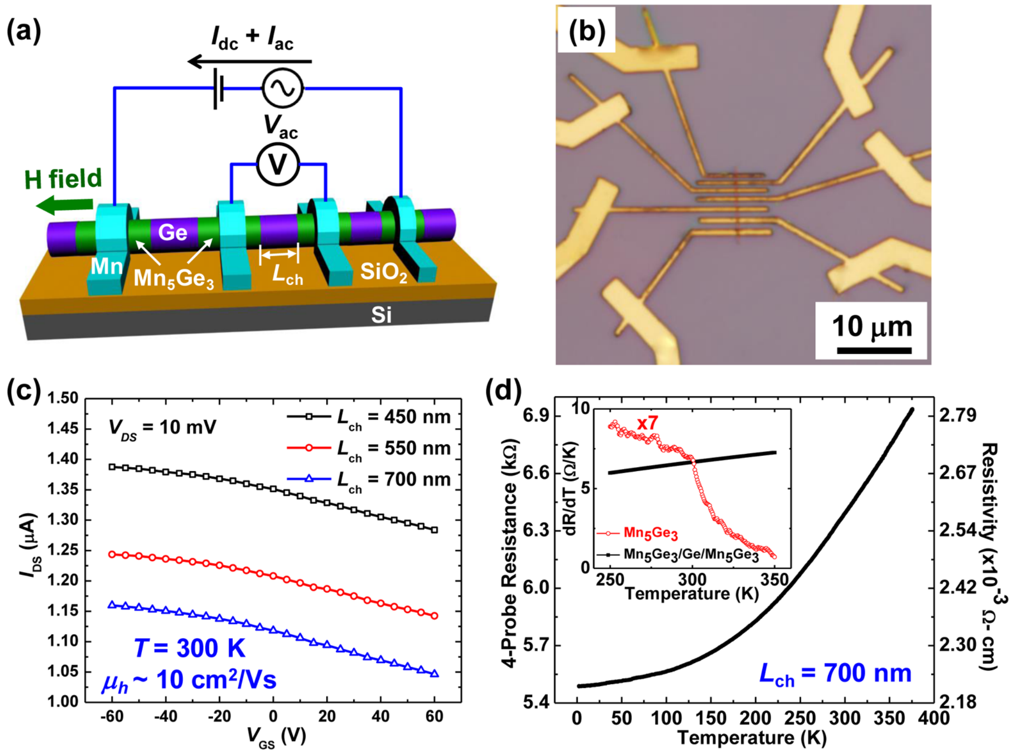

Figure 1. Characterization of single-crystalline $Mn_5Ge_3/Ge/Mn_5Ge_3$ nanowire transistors. (a) Schematic illustration of Ge nanowire transistors with thermally formed Mn_5Ge_3 as Schottky source/drain contacts. The setup for a standard 4-probe measurement is also illustrated. The magnetic field for the following measurements in this study was applied along the nanowire axial direction. (b) Optical microscope image of multiple as-fabricated $Mn_5Ge_3/Ge/Mn_5Ge_3$ nanowire transistors on a SiO_2/Si substrate. (c) $I_{DS}-V_{GS}$ curves of three Ge nanowire transistors with different channel lengths (L_{ch} = 450, 550, and 700 nm) with V_{DS} = 10 mV, showing a p-type transistor behavior with a field-effect hole mobility of about 10 cm²/(V s). (d) The 4-probe resistance-temperature (R-T) measurement on the $Mn_5Ge_3/Ge/Mn_5Ge_3$ nanowire transistor with a channel length of L_{ch} = 700 nm, showing a decreasing resistance with the decreasing temperature. This confirms the degenerate indium doping in the Ge nanowire. The inset shows the first-order derivative of the R-T curve (black curve), showing a smooth transition near T = 300 K. For comparison, the data of a Mn_5Ge_3 nanowire (red curve, multiplied by a factor of 7) adopted from ref 24 is also plotted here.

scatterings;[3,17] (3) while the insertion of a tunneling or Schottky barrier helps alleviate the conductivity mismatch,[18,19] the preparation of a high-quality tunneling oxide without pinholes or a defects-free Schottky contact without Fermi-level pinning is not easy.[20,21] Also, the localized states at the FM/SC interface and the surface roughness could significantly complicate and jeopardize the spin injection process.[22] Therefore, the preparation of high-quality FM/SC structures is a key step toward realizing efficient spin injection into semiconductors. In an earlier work, we were able to fabricate single-crystalline $Mn_5Ge_3/Ge/Mn_5Ge_3$ nanowire transistors using a simple rapid thermal annealing (RTA) process[23] in which the formed Mn_5Ge_3 Schottky contacts maintained atomically clean interfaces with Ge nanowires and the Mn_5Ge_3 nanowire exhibited ferromagnetic orderings up to room temperature.[24] It should be pointed out that the Curie temperature of Mn_5Ge_3 can be further increased up to 445 K with appropriate carbon doping in order to build practical spintronic devices that can operate at room temperature.[25] Moreover, such one-dimensional high-quality germanide/Ge contacts formed by RTA were found to effectively alleviate the Fermi level pinning,[26] for which conventional metal/Ge contacts were suffered.[27] This should allow us to probe the intrinsic spin property in the $Mn_5Ge_3/Ge/Mn_5Ge_3$ nanowire transistor. Indeed, with a high spin polarization,[28] Mn_5Ge_3 has been theoretically predicted to be a high-efficiency spin injection source into Ge.[29] In this work, we demonstrate the spin injection into Ge nanowires through Mn_5Ge_3 source/drain contacts in $Mn_5Ge_3/Ge/Mn_5Ge_3$ nanowire transistors. We also study the bias effect and the temperature dependence of the spin transport, revealing a weak temperature dependence for the spin diffusion length of about 480 nm and the spin lifetime exceeding 244 ps in degenerately p-doped Ge nanowires. These numbers in Ge nanowires are much larger than those reported in bulk Ge with a similar doping level,[30] which can be attributed to the significant suppression of spin relaxation because of quantum confinements in nanostructures.

Results and Discussion. Single-crystalline Mn_5Ge_3/Ge/Mn_5Ge_3 nanowire transistors were fabricated on a Ge nanowire with Mn metal contacts using a RTA process, as described in a prior work for the formation of ferromagnetic source/drain contacts in Ge nanowire transistors.[23] Figure 1a schematically illustrates the device structure, in which the ferromagnetic Mn_5Ge_3 nanowire contacts were formed upon 450 °C RTA. The formed Mn_5Ge_3/Ge heterostructure with an atomically clean interface provides a defects-free FM/SC structure for electrical spin injection. The Schottky barrier for the Mn_5Ge_3 contact to a p-type Ge nanowire was determined to be about 0.25 eV from temperature-dependent $I-V$ measurements.[23] To overcome the fundamental obstacle of conductivity mismatch,[16] heavily doped Ge nanowires were required to achieve appreciable spin injection from the ferromagnetic Mn_5Ge_3 contact into the Ge nanowire. In the previous work, as-grown Ge nanowires were not intentionally doped during the vapor–

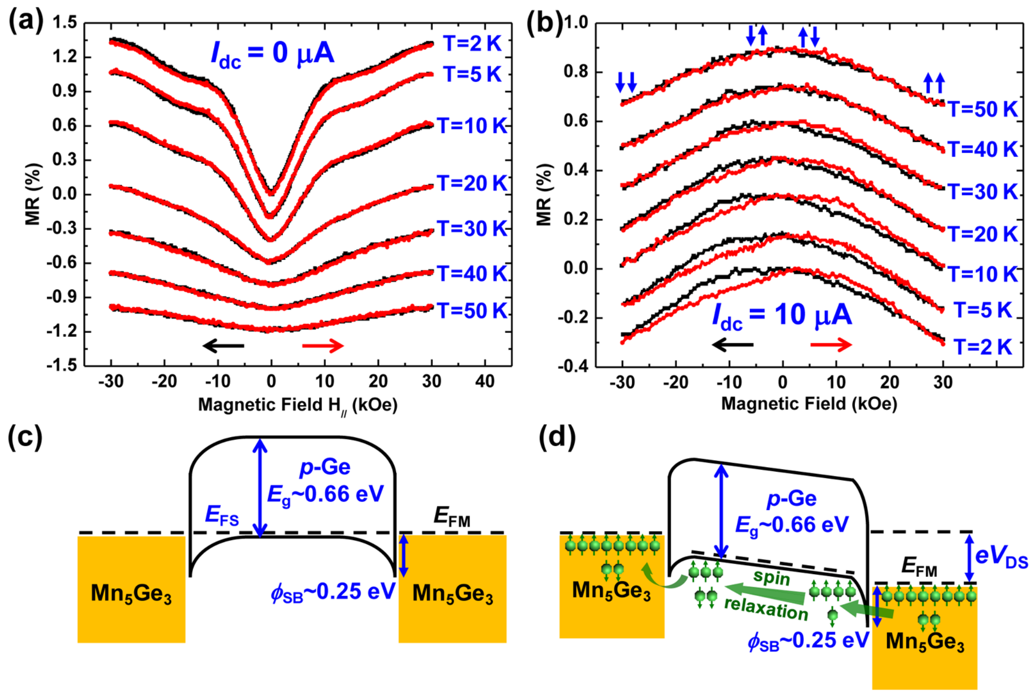

Figure 2. MR loops of a Mn_5Ge_3/Ge/Mn_5Ge_3 nanowire transistor with a channel length of L_{ch} = 700 nm at different temperatures from 2 to 50 K under a dc current bias of (a) I_{dc} = 0 μA and (b) I_{dc} = 10 μA, respectively. The black and red arrows indicate the backward and forward sweeping directions of the axial magnetic field between −30 and 30 kOe, respectively. For clarity, MR curves in (a) and (b) are intentionally offset by multiples of 0.2 and 0.15%, respectively. The Mn_5Ge_3/Ge/Mn_5Ge_3 nanowire transistor showed positive MR curves with no apparent hysteresis under zero dc bias (I_{dc} = 0 μA) while negative and hysteretic MR curves under a large dc bias (I_{dc} = 10 μA). The blue arrows in (b) indicate the relative magnetization directions of the Mn_5Ge_3 spin injector and the spin detector. Energy band diagrams of the Mn_5Ge_3/Ge/Mn_5Ge_3 nanowire transistor under zero and large dc bias are shown in (c,d), respectively. The transport process of spin-polarized carriers (holes) in the Mn_5Ge_3/Ge/Mn_5Ge_3 nanowire transistor is also illustrated in (d).

liquid–solid growth process.[31] Here in order to introduce a high doping density, as-grown Ge nanowires were exposed in an indium ambient at about 600 °C inside an ultrahigh-vacuum molecular beam epitaxy (MBE) chamber for 2 hours to drive indium atoms diffusing into Ge nanowires as p-type dopants, prior to being transferred onto SiO_2/Si substrates for device fabrication. The Ge nanowire morphology was inspected with transmission electron microscope (TEM) to ensure that the Ge nanowire maintained the cubic crystal structure after incorporating indium doping (see Figure S1 in Supporting Information). Furthermore, the energy-dispersive X-ray spectrum (EDS, with a resolution of about 0.1% atomic concentration) of indium-doped Ge nanowires revealed a very small peak of indium, affirming the successful incorporation of indium dopants into the Ge lattice (see Figure S2 in Supporting Information).

Figure 1b shows the optical microscope image of multiple as-fabricated Mn_5Ge_3/Ge/Mn_5Ge_3 nanowire transistors after transferring indium-doped Ge nanowires onto a SiO_2/Si substrate. No scanning electron microscope (SEM) image was taken to avoid undesirable damages on the device by the high-energy electron beam; however it was expected to be similar to the prior work.[23] The Si substrate was degenerately doped and used as a back-gate electrode while the 300 nm thick SiO_2 layer grown on top by thermal oxidization served as the gate dielectric. Figure 1c shows the I_{DS}−V_{GS} curves of three Mn_5Ge_3/Ge/Mn_5Ge_3 nanowire transistors with different channel lengths (L_{ch} = 450, 550, and 700 nm) under V_{DS} = 10 mV measured in the room-temperature ambient (see Figure S3 in Supporting Information for the detailed device dimensions). They all showed a similar p-type transistor behavior with a field-effect hole mobility of about μ_h = 10 cm^2/(V s), which was calculated from the transconductance as discussed in prior works.[32−34] It was noted that the Ge nanowire transistors showed about 1 order of magnitude improvement in the carrier mobility after RTA at 450 °C (see Figure S4 in Supporting Information), and such an improvement was attributed to the formation of high-quality Mn_5Ge_3 source/drain contacts after annealing.[33] Compared with the reported performance of Mn_5Ge_3/Ge/Mn_5Ge_3 nanowire transistors built on as-grown Ge nanowires,[23] the devices here showed a much lower hole mobility and a smaller current on/off ratio while with a higher nanowire conductance. This result implied a high concentration of indium doping in the Ge nanowire due to the fact that it is difficult to deplete a heavily doped semiconductor and the high-concentration dopants drastically degrade the carrier mobility through impurity scatterings.[35] To quantitatively evaluate the Ge nanowire resistivity and the indium doping concentration, temperature-dependent resistance measurements were performed on a Mn_5Ge_3/Ge/Mn_5Ge_3 nanowire transistor with a channel length of L_{ch} = 700 nm and with a diameter of about 60 nm. A standard 4-probe measurement setup with a lock-in technique was used to exclude the contact resistance and improve the signal-to-noise ratio in the measurement. The measurement setup is illustrated in Figure 1a. As shown in Figure 1d, the Mn_5Ge_3/Ge/Mn_5Ge_3 nanowire transistor exhibited a monotonically decreasing resistance with decreasing temperature down to T = 2 K. This behavior reaffirmed the degenerate doping in the Ge nanowire in which case the dominated

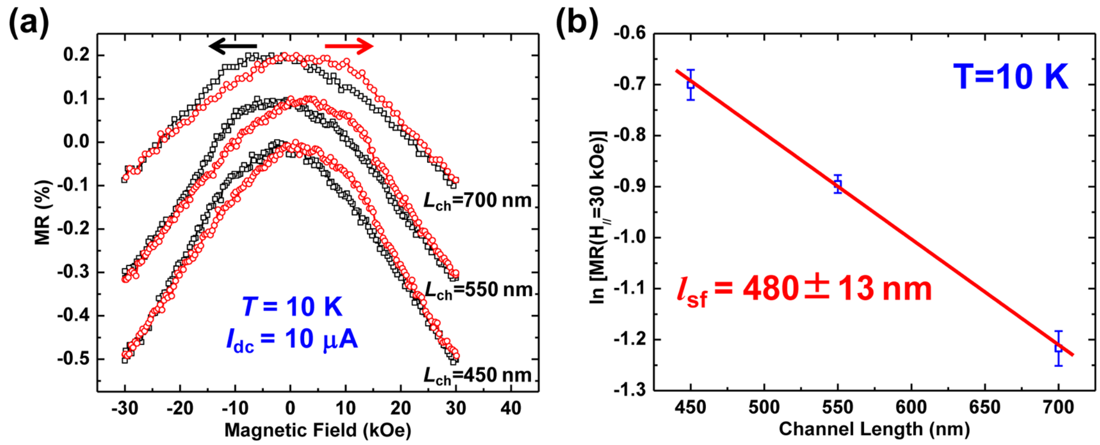

Figure 3. (a) MR curves of three Mn_5Ge_3/Ge/Mn_5Ge_3 nanowire transistor with three different channel lengths (L_{ch} = 450, 550, and 700 nm) at T = 10 K under a dc current bias of I_{dc} = 10 μA. The black and red arrows indicate the backward and forward sweeping directions of the axial magnetic field between −30 and 30 kOe, respectively. All the MR curves are intentionally offset by multiples of 0.1% for clarity. (b) Semilog plot of the MR magnitude at $H_{//}$ = 30 kOe versus the channel length for the three Mn_5Ge_3/Ge/Mn_5Ge_3 nanowire transistors. The linear fitting (red curve) yields a spin diffusion length of l_{sf} = 480 ± 13 nm in the p-type Ge nanowire at T = 10 K.

impurity scattering was effectively screened by the high-density free carriers.[36] The first-order derivative of the 4-probe resistance with respect to the temperature (dR/dT) was also plotted in the inset of Figure 1d, showing a smooth change from 250 to 350 K for the Mn_5Ge_3/Ge/Mn_5Ge_3 nanowire transistor. Compared with the clear cusp in the dR/dT curve near T_C =300 K for the Mn_5Ge_3 nanowire in ref 24 (also replotted in the inset of Figure 1d for comparison),[24] this result suggested that the part of the resistance from the Mn_5Ge_3 source/drain was small and most of the measured resistance came from the Ge nanowire channel. Quantitatively, using the previously measured resistivity value for the Mn_5Ge_3 nanowire,[24] we calculated that the Mn_5Ge_3 contacts only contributed to less than 3% of the total Mn_5Ge_3/Ge/Mn_5Ge_3 resistance. Therefore, for simplicity, we assumed the measured total resistance equaled to the Ge nanowire channel resistance. Then the resistivity of the Ge channel was calculated to be ρ_{Ge} = 2.58 × 10^{-3} Ω-cm at T = 300 K and decreased slightly to ρ_{Ge} = 2.22 × 10^{-3} Ω-cm at T = 2 K. On the other hand, the previously reported resistivity values for the Mn_5Ge_3 nanowire were ρ_{FM} = 2.4 × 10^{-4} Ω-cm at T = 300 K and decreased to ρ_{FM} = 4.65 × 10^{-5} Ω-cm at T = 2 K.[24] The conductivity ratio (inversely the resistivity ratio), $\sigma_{FM}/\sigma_{Ge} = \rho_{Ge}/\rho_{FM}$, of the Mn_5Ge_3/Ge heterostructure was then evaluated to be between 10 and 50 in the temperature range of 2−300 K. This value is more than 20 times smaller than that of ordinary FM/Ge (e.g., Fe/Ge, Co/Ge) spin injection structures, given that the resistivity of commonly used ferromagnetic metals is typically on the order of 10^{-6} to 10^{-5} Ω-cm, or at least 20 times lower than that of Mn_5Ge_3.[37] Therefore, compared with ordinary FM/Ge structures, the conductivity mismatch in the Mn_5Ge_3/Ge/Mn_5Ge_3 nanowire transistor should be significantly reduced to facilitate the spin injection into Ge. It is also worth mentioning that the spin polarization in Mn_5Ge_3 was experimentally reported to be about P_{FM} = 42% at T = 1.2 K,[28] which is comparable with that of conventional ferromagnetic metals (for instance, P_{Fe} = 45%, P_{Co} = 42%, and P_{Ni} = 33%).[38] The relatively low conductivity and high spin polarization of Mn_5Ge_3, along with the atomically clean interfaces with Ge nanowires, suggests that Mn_5Ge_3 is a promising ferromagnetic material for spin injection into Ge nanowires.

In the characterization of spin injection and transport, Hanle precession measurement is widely used to extract the spin lifetime and spin diffusion length.[15] Usually nonlocal measurements with a four-terminal geometry are adopted to detect the intrinsic spin injection signal in order to avoid any spurious signals.[39] Unfortunately, this technique could not be used for our Mn_5Ge_3/Ge/Mn_5Ge_3 nanowire transistor (see Figure S5 in Supporting Information for detailed explanation). Alternatively, we may use the Mn_5Ge_3/Ge/Mn_5Ge_3 nanowire transistor as a vertical spin valve with a current perpendicular-to-plane configuration.[40,41] In this case, spin-polarized carriers are injected into the Ge nanowire from one ferromagnetic Mn_5Ge_3 contact (namely the spin injector) and then are scattered as they travel along the Ge nanowire channel before reaching the other ferromagnetic Mn_5Ge_3 contact (namely the spin detector). This process will be discussed in details later (illustrated in Figure 2d). For nonpolar semiconductors like Ge, the dominant spin relaxation mechanism is the Elliot-Yafet spin flip mechanism that occurs when scattered with phonons and impurities.[3] In experiment, a constant dc bias current superimposed with a small ac current of I_{ac} = 1 μA was flowed through the Mn_5Ge_3/Ge/Mn_5Ge_3 nanowire transistor, and the ac voltage signal was sensed with standard lock-in technique while sweeping the axial magnetic field. The easy-axis of the Mn_5Ge_3 nanowire was found to be along the nanowire axis, and the two ferromagnetic Mn_5Ge_3 contacts were intentionally designed to have different lengths and hence possibly different coercive fields. As the axial magnetic field was swept back and forth between −30 and 30 kOe, the relative magnetization directions of the spin injector and the spin detector were changed between parallel and antiparallel configurations. Figure 2a,b shows the MR of a Mn_5Ge_3/Ge/Mn_5Ge_3 nanowire transistor with a channel length of L_{ch} = 700 nm under two different dc current biases in the temperature range from 2 to 50 K. The MR here is defined as MR = $((R(H) - R_{min})/R_{min})$ × 100% (positive MR) for Figure 2a, and MR = $((R(H) - R_{max})/R_{max})$ × 100% (negative MR) for Figure 2b. It is interesting to observe that the MR curves under a zero and a high dc bias current showed distinct characteristics: positive MR with no apparent hysteresis with I_{dc} = 0 μA while there is a negative and hysteretic MR under I_{dc} = 10 μA. It should be pointed out that while the positive MR under I_{dc} = 0 μA is likely attributed to the longitudinal MR of Ge,[42] the bias-dependent MR characteristics could not originate from the Ge nanowire, the Mn_5Ge_3 contact, and associated anisotropy magnetoresistance (see Figure S6 in Supporting Information for detailed explanation). The bias effect on the MR behavior can be simply explained from the energy band diagram schematically shown in Figures 2c,d: since there is a Schottky barrier height of about 0.25 eV for the ferromagnetic Mn_5Ge_3 contact to the p-type Ge nanowire,[23] a large enough dc bias voltage (current) is required to reduce the Schottky barrier width in the reverse biased spin injector terminal to allow for sufficient spin-polarized carriers being injected into the Ge nanowire channel and moving toward the spin detector. The transport process of spin-polarized carriers in the Mn_5Ge_3/Ge/Mn_5Ge_3 nanowire transistor is also schematically illustrated in Figure 2d. As shown in Figure 2b, with a dc current bias of I_{dc} = 10 μA we were able to observe the negative and hysteretic MR from T = 2 K up to T = 50 K, unambiguously demonstrating the spin injection and detection in the Ge nanowire transistor. More MR curves are shown in the Supporting Information (see Figure S7 in Supporting Information). It is worth noting that similar bias effect on the MR behavior was also observed in the MnSi/Si/MnSi nanowire heterostructure in which spin-polarized carriers were injected from the Schottky MnSi contact into the p-type Si nanowire.[43]

To quantitatively determine the spin diffusion length, temperature-dependent MR measurements were performed on several Mn_5Ge_3/Ge/Mn_5Ge_3 nanowire transistors with different channel lengths. Figure 3a shows the MR curves of three Mn_5Ge_3/Ge/Mn_5Ge_3 nanowire transistors with three different channel lengths (L_{ch} = 450, 550, and 700 nm) at T = 10 K under the same dc current bias of I_{dc} = 10 μA. They showed similar negative and hysteretic characteristics with a systematic decrease in the MR magnitude with the increasing Ge nanowire channel length. Recalling the Julliere's model for a FM/insulator/FM structure,[44] the tunneling magnetoresistance (TMR) is given by

$$\mathrm{TMR} = \frac{2P_1P_2}{1 + P_1P_2} \tag{1}$$

Here P_1 and P_2 are the spin polarizations of the two FM electrodes defined as $P = (N_\uparrow - N_\downarrow)/(N_\uparrow + N_\downarrow)$ in which $N_\uparrow$ ($N_\downarrow$) is the density of states at the Fermi level for the majority (minority) spin direction. In our Mn_5Ge_3/Ge/Mn_5Ge_3 nanowire structure with a fairly long Ge channel, the Julliere's model of TMR can be modified as follows to include the spin relaxation in the Ge nanowire[41]

$$\mathrm{TMR} = \frac{2P_1P_2e^{-L_{ch}/l_{sf}}}{1 + P_1P_2e^{-L_{ch}/l_{sf}}} \tag{2}$$

where L_{ch} is the Ge nanowire channel length, and l_{sf} is the spin diffusion length (see Figure S8 in Supporting Information for more discussions on the model). In the case where $P_1P_2e^{-(L/\mathrm{lsf})} \ll 1$, or equivalently the TMR magnitude is small (such as in this work), eq 2 can be further simplified as an exponential function

$$\mathrm{TMR} \approx 2P_1P_2e^{-L_{ch}/l_{sf}} \tag{3}$$

In the MR curves of Mn_5Ge_3/Ge/Mn_5Ge_3 nanowire transistors shown in Figure 3a, it is difficult to accurately determine the TMR magnitude, because typical abrupt resistance steps were not observed as in previous organic spin valves that comprised two different ferromagnetic contacts.[40,41] This could be attributed to a possibly small difference in the coercive field for the Mn_5Ge_3 spin injector and detector (with the same diameter but slightly different lengths). In addition, the presence of multiple domains in the ferromagnetic Mn_5Ge_3 nanowire would also prevent the abrupt switching of its magnetization.[24] Further investigation may be required to understand the detailed mechanism. Here, in order to extract the spin diffusion length in the Ge nanowire, we obtained the MR amplitude of three Mn_5Ge_3/Ge/Mn_5Ge_3 nanowire transistors with different L_{ch} at the same temperature and magnetic field. Here we picked the largest magnetic field in our measurements to ensure the magnetization of all the Mn_5Ge_3 nanowires in parallel. The rationale is to compare the MR ratio of three Mn_5Ge_3/Ge/Mn_5Ge_3 nanowire transistors with different Ge nanowire channel lengths while keeping all other parameters the same (same temperature and bias condition, etc.). Therefore, the change in the MR ratio should closely related to the spin relaxation in the Ge nanowire. A semilog plot of the MR magnitude at $H_{//}$ = 30 kOe versus the channel length is then plotted at T = 10 K in Figure 3b. Using eq 3, one yields a spin diffusion length of l_{sf} = 480 ± 13 nm in the p-type Ge nanowire at T = 10 K. To make a meaningful comparison with previous results in Ge, we first estimated the doping concentration in our Ge nanowires. Using the resistivity-doping concentration relation in bulk Ge as an approximation,[45] the resistivity value of ρ_{Ge} = 2.58 × 10^{-3} Ω-cm at T = 300 K corresponds to a p-type doping concentration of about N_A = 8 × 10^{18} cm^{-3}. Measurements from more than 10 devices yielded a p-doping concentration in the range between 6 × 10^{18} and 9 × 10^{18} cm^{-3}. From the literature,[30] p-type bulk Ge with a similar doping concentration of N_A = 8.2 × 10^{18} cm^{-3} was reported to have a spin diffusion length of about l_{sf} = 80 nm (calculated at T = 300 K but it is also valid for temperature down to T = 5 K as both the spin lifetime τ_{sf} and the diffusion constant D_h have a weak temperature dependence in heavily doped semiconductors[17,30,46]). The significant enhancement in the spin diffusion length in the one-dimensional Ge nanowire channel could be attributed to the effective suppression of electron−phonon scattering and thus spin relaxation by quantum confinements in nanostructures with a reduced density of states.[47] From eq 3, we can also extract the spin polarization of Mn_5Ge_3 to be about 8% at T = 10 K, which is much smaller than the reported (42 ± 5)% at T = 1.2 K from point contact Andreev reflection measurements.[28] This large deviation is mainly because that the simplified TMR model here does not include the spin injection efficiency from Mn_5Ge_3 into Ge (see Figure S8 in Supporting Information for more discussions).

To estimate the spin lifetime, we first calculated the diffusion constant, which can be obtained in degenerately doped semiconductors using the full Fermi-Dirac expression[35]

$$D_h = \frac{2\mu_h k_B T}{q}\frac{F_{1/2}(\eta_F)}{F_{-1/2}(\eta_F)} \tag{4}$$

in which μ_h is the hole mobility, k_B is the Boltzmann constant, q is the electron charge, $\eta_F = (E_V - E_F)/k_BT$ while $F_{1/2}(\eta_F)$ and $F_{-1/2}(\eta_F)$ are the Fermi-Dirac integrals. The Fermi-level position in degenerate semiconductors can be determined using the Joyce-Dixon approximation[48]

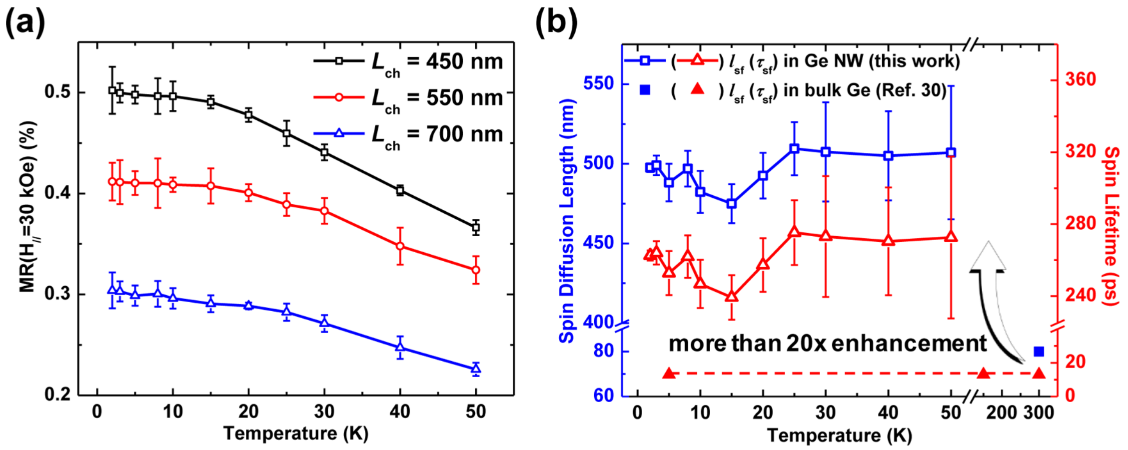

Figure 4. (a) Temperature-dependent MR magnitudes at $H_{//}$ = 30 kOe for three Mn_5Ge_3/Ge/Mn_5Ge_3 nanowire transistors with different channel lengths (L_{ch} = 450, 550, and 700 nm) under a dc current bias of I_{dc} = 10 μA, showing a similar temperature dependence. (b) Fitted temperature-dependent spin diffusion length and calculated spin lifetime, showing a weak dependence on the temperature from 2 to 50 K. The apparent dip at 10 K is likely due to the fitting error. For comparison, the data from bulk Ge with a similar p-type doping concentration in ref 30 are also included and represented by solid symbols. Ge nanowires showed more than 20 times enhancement in the spin diffusion length and spin lifetime compared with bulk Ge.

$$E_V - E_F \approx k_B T\left(\ln\frac{N_A}{N_V} + 2^{-1.5}\times\frac{N_A}{N_V}\right) \quad (5)$$

Using the measured field-effect hole mobility of μ_h = 10 cm^2/(V s) at T = 300 K we can calculate the diffusion constant to be D_h = 0.377 cm^2/s given $N_A = 8 \times 10^{18}$ cm^{-3} and $N_V = 6 \times 10^{18}$ cm^{-3}.[35] As the diffusion constant is weakly dependent on the temperature,[17,30] we assume the same value for low temperatures so we can further estimate the spin lifetime at T = 10 K using

$$\tau_{sf} = \frac{{l_{sf}}^2}{D_h} = 6.11\ \text{ns} \quad (6)$$

It is recognized that the mobility value extracted from the I_{DS}–V_{GS} curves may underestimate the conductivity mobility considering the back-gated device structure and the round shape of Ge nanowires.[23] Therefore, the above-calculated τ_{sf} = 6.11 ns is the upper limit for the spin lifetime. If we adopt the reported hole mobility of μ_h = 250 cm^2/(V s) from a p-type Ge thin film with a similar doping concentration,[30] eq 6 would yield the lower limit for the spin lifetime of about τ_{sf} = 244 ps with D_h = 9.43 cm^2/s. Still this value is 1 order of magnitude larger than that observed in bulk Ge,[30] again implying the advantage of low-dimensional nanostructures in the building of spintronic devices with long spin lifetime and spin diffusion length.[47]

Furthermore, to investigate the temperature dependence of the spin diffusion length, we obtained the temperature-dependent MR magnitudes at $H_{//}$ = 30 kOe for three Mn_5Ge_3/Ge/Mn_5Ge_3 nanowire transistors with different channel lengths (L_{ch} = 450, 550, and 700 nm) as shown in Figure 4a. Their MR magnitudes showed a similar temperature dependence: the MR magnitude linearly increases with reducing temperature from T = 50 K and then gradually saturates as the temperature went below T = 10 K. Using eq 3, we obtained the temperature-dependent spin diffusion length as given in Figure 4b, showing a weak temperature dependence of the spin diffusion length in the range of T = 2 K to T = 50 K. The calculated spin lifetime at each temperature using eq 6 is also plotted, assuming a constant diffusion constant of D_h = 9.43 cm^2/s. Such a weak temperature dependence of the spin diffusion length and lifetime was also observed in heavily doped Si thin films.[17,46] This fact may be explained by the effectively screened ionized impurity scatterings in the heavily doped Ge nanowire,[36] resulting in a weak dependence on the temperature for the momentum relaxation and hence the spin relaxation (as manifested by the spin diffusion length and the spin lifetime). For comparison, the data from Ge thin films with a similar p-type doping concentration in ref 30 are also included in Figure 4b, manifesting the significant enhancement of the spin diffusion length and lifetime in Ge nanostructures.[47]

Conclusions. To sum up, we have successfully demonstrated electrical spin injection and detection in single-crystalline Mn_5Ge_3/Ge/Mn_5Ge_3 nanowire transistors fabricated on degenerately indium-doped Ge nanowires. Under zero current bias, the Mn_5Ge_3/Ge/Mn_5Ge_3 nanowire transistor showed positive and symmetric MR characteristics with no apparent hysteresis; on the other hand, negative and hysteretic MR characteristics were observed under a large voltage (current) bias from T = 2 K up to T = 50 K. The hysteretic MR signature clearly indicated spin injection from the ferromagnetic Mn_5Ge_3 contact into the Ge nanowire, and the large bias helped reduce depletion region width of the Mn_5Ge_3/Ge junction to increase the spin injection efficiency. Furthermore, based on the modified Julliere's model, the MR of three Mn_5Ge_3/Ge/Mn_5Ge_3 nanowire transistors gave a spin diffusion length of l_{sf} = 480 ± 13 nm and a long spin lifetime exceeding 244 ps in p-type Ge nanowires at T = 10 K. The estimated spin diffusion length is significantly larger than the channel length of state-of-the-art MOS transistors[1] and has a weak temperature dependence. The long spin diffusion length and its weak temperature dependence were explained by the dominant Elliot-Yafet spin-relaxation mechanism as the result of the impurity scatterings in Ge, which were effectively screened in degenerately doped semiconductors. These observed spin diffusion length and spin lifetime in one-dimensional Ge nanowires were much larger than those reported from bulk Ge,[30] which implied that the spin relaxation can be effectively suppressed in the one-dimensional channel because of the quantum confinement effect.[9,47]

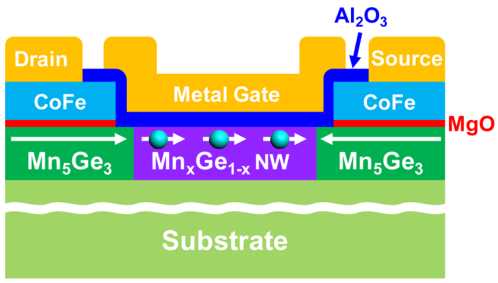

Figure 5. Schematic illustration of a nonvolatile transpinor device, which is built on a Mn_xGe_{1-x} DMS nanowire with ferromagnetic Mn_5Ge_3 contacts. Another choice for the source/drain contacts could be Co(Fe)/MgO tunnel junctions. The CoFe/MgO magnetic tunnel junctions are used to read out/manipulate the magnetization of the Mn_5Ge_3 nanomagnets. Other strategies could involve spin valve structures or the inverse spin Hall effect. The ferromagnetism of the Mn_xGe_{1-x} DMS nanowire channel can be controlled by the gate electric field. The magnetic moments are transferred from the source to the channel and then to the drain.

With a relatively long spin diffusion length and the convenient fabrication process for $Mn_5Ge_3/Ge/Mn_5Ge_3$ nanowire transistors, it is possible to integrate Ge nanowire-based spintronic devices into standard CMOS technology. With spin-based transistors, this may help create novel functional devices with low power dissipation and fast switching. One promising prototype, as shown in Figure 5, is to integrate a diluted magnetic semiconductor (DMS) nanowire, whose ferromagnetism can be effectively controlled by a gate electrode, with the high-quality ferromagnetic contacts for spin injection demonstrated in this work. Another variant of the ferromagnetic source/drain contacts could be Co(Fe)/MgO tunnel junctions for spin injection.[9] Our previous work has successfully demonstrated the electric field control of ferromagnetism in Mn-doped Ge DMS quantum dots up to 300 K,[49,50] and similar effect is expected in Mn_xGe_{1-x} DMS nanowires. In this spin-based transistor (transpinor), the information is stored as the magnetization of the ferromagnetic Mn_5Ge_3 contacts (nanomagnets), and it can be read out and manipulated by a magnetic tunnel junction that converts the spin signal into a current/voltage signal. Other conversion strategies may involve spin valve structures or the inverse spin Hall effect.[51] The magnetic moments are transferred from the source to the channel and then to the drain through spin injection and exchange interaction. As the electric field exerted by the gate electrode manipulates the ferromagnetism in the DMS channel, the gate controls the communication between the source/drain terminals. This DMS nanowire-based transpinor points out a possible realization of all-spin logic devices with built-in memory for low-power operations.[52]

■ ASSOCIATED CONTENT

Ⓢ Supporting Information

TEM image and diffraction pattern of indium-doped Ge nanowires; EDS spectrum of indium-doped Ge nanowires; schematic of device dimensions; $I_{DS}-V_{GS}$ curves of Mn_5Ge_3/Ge/Mn_5Ge_3 nanowire transistors before and after RTA; discussion on nonlocal measurements; temperature-dependent MR curves of $Mn_5Ge_3/Ge/Mn_5Ge_3$ nanowire transistors; and discussion on Mn_5Ge_3 spin polarization. This material is available free of charge via the Internet at http://pubs.acs.org.

■ AUTHOR INFORMATION

Corresponding Author

*E-mail: (K.L.W.) wang@ee.ucla.edu; (L.J.C.) ljchen@mx.nthu.edu.tw.

Author Contributions

‖J.T. and C.-Y.W. contributed equally.

Notes

The authors declare no competing financial interest.

■ ACKNOWLEDGMENTS

This work was in part supported by Western Institution of Nanoelectronics (WIN) and the Focus Center on Functional Engineered Nano Architectonics (FENA). The authors also acknowledged the support from National Science Council through Grant NSC 101-2221-E-007-078, NSC 102-2221-E-007-023-MY3, NSC 102-2221-E-007-090-MY2, and NSC 101-2623-E-007-013-IT, the Ministry of Economic Affairs, Taiwan (101-EC-17-A-09-S1-198), National Tsing Hua University (100N2060E1, 100N2041E1), and the assistance from Center for Energy and Environmental Research, National Tsing Hua University.

■ REFERENCES

(1) *International Technology Roadmap of Semiconductors*, 2012 ed.; http://www.itrs.net; accessed Jan 21, 2013.
(2) Wolf, S. A.; Awschalom, D. D.; Buhrman, R. A.; Daughton, J. M.; Molnar, S. v.; Roukes, M. L.; Chtchelkanova, A. Y.; Treger, D. M. Spintronics: A Spin-Based Electronics Vision for the Future. *Science* **2001**, *294*, 1488−1495.
(3) Žutić, I.; Fabian, J.; Das Sarma, S. Spintronics: Fundamentals and Applications. *Rev. Mod. Phys.* **2004**, *76*, 323−410.
(4) Datta, S.; Das, B. Electronic Analog of the Electro-Optic Modulator. *Appl. Phys. Lett.* **1990**, *56*, 665−667.
(5) Sugahara, S.; Tanaka, M. A Spin Metal-Oxide-Semiconductor Field-Effect Transistor using Half-Metallic-Ferromagnet Contacts for the Source and Drain. *Appl. Phys. Lett.* **2004**, *84*, 2307−2309.
(6) Jonker, B. T.; Kioseoglou, G.; Hanbicki, A. T.; Li, C. H.; Thompson, P. E. Electrical Spin-Injection into Silicon from a Ferromagnetic Metal/Tunnel Barrier Contact. *Nat. Phys.* **2007**, *3*, 542−546.
(7) Dash, S. P.; Sharma, S.; Patel, R. S.; de Jong, M. P.; Jansen, R. Electrical Creation of Spin Polarization in Silicon at Room Temperature. *Nature* **2009**, *462*, 491−494.
(8) Zhou, Y.; Han, W.; Chang, L.-T.; Xiu, F.; Wang, M.; Oehme, M.; Fischer, I. A.; Schulze, J.; Kawakami, R. K.; Wang, K. L. Electrical Spin Injection and Transport in Germanium. *Phys. Rev. B* **2011**, *84*, 125323.
(9) Liu, E.-S.; Nah, J.; Varahramyan, K. M.; Tutuc, E. Lateral Spin Injection in Germanium Nanowires. *Nano Lett.* **2010**, *10*, 3297−3301.
(10) Lou, X.; Adelmann, C.; Crooker, S. A.; Garlid, E. S.; Zhang, J.; Reddy, K. S. M.; Flexner, S. D.; Palmstrom, C. J.; Crowell, P. A. Electrical Detection of Spin Transport in Lateral Ferromagnet-Semiconductor Devices. *Nat. Phys.* **2007**, *3*, 197−202.
(11) Zhu, H. J.; Ramsteiner, M.; Kostial, H.; Wassermeier, M.; Schönherr, H.-P.; Ploog, K. H. Room-Temperature Spin Injection from Fe into GaAs. *Phys. Rev. Lett.* **2001**, *87*, 016601.
(12) Tombros, N.; Jozsa, C.; Popinciuc, M.; Jonkman, H. T.; van Wees, B. J. Electronic Spin Transport and Spin Precession in Single Graphene Layers at Room Temperature. *Nature* **2007**, *448*, 571−574.
(13) Han, W.; Pi, K.; McCreary, K. M.; Li, Y.; Wong, J. J. I.; Swartz, A. G.; Kawakami, R. K. Tunneling Spin Injection into Single Layer Graphene. *Phys. Rev. Lett.* **2010**, *105*, 167202.
(14) Jedema, F. J.; Filip, A. T.; van Wees, B. J. Electrical Spin Injection and Accumulation at Room Temperature in an All-Metal Mesoscopic Spin Valve. *Nature* **2001**, *410*, 345−348.

(15) Jedema, F. J.; Heersche, H. B.; Filip, A. T.; Baselmans, J. J. A.; van Wees, B. J. Electrical Detection of Spin Precession in a Metallic Mesoscopic Spin Valve. *Nature* **2002**, *416*, 713−716.
(16) Schmidt, G.; Ferrand, D.; Molenkamp, L. W.; Filip, A. T.; van Wees, B. J. Fundamental Obstacle for Electrical Spin Injection from a Ferromagnetic Metal into a Diffusive Semiconductor. *Phys. Rev. B* **2000**, *62*, R4790−R4793.
(17) Li, C. H.; van 't Erve, O. M. J.; Jonker, B. T. Electrical Injection and Detection of Spin Accumulation in Silicon at 500 K with Magnetic Metal/Silicon Dioxide Contacts. *Nat. Commun.* **2011**, *2*, 245.
(18) Fert, A.; Jaffrès, H. Conditions for Efficient Spin Injection from a Ferromagnetic Metal into a Semiconductor. *Phys. Rev. B* **2001**, *64*, 184420.
(19) Rashba, E. I. Theory of Electrical Spin Injection: Tunnel Contacts as a Solution of the Conductivity Mismatch Problem. *Phys. Rev. B* **2000**, *62*, R16267−R16270.
(20) Han, W.; Zhou, Y.; Wang, Y.; Li, Y.; Wong, J. J. I.; Pi, K.; Swartz, A. G.; McCreary, K. M.; Xiu, F.; Wang, K. L.; Zou, J.; Kawakami, R. K. Growth of Single-Crystalline, Atomically Smooth MgO Films on Ge(001) by Molecular Beam Epitaxy. *J. Cryst. Growth* **2009**, *312*, 44−47.
(21) Yamane, K.; Hamaya, K.; Ando, Y.; Enomoto, Y.; Yamamoto, K.; Sadoh, T.; Miyao, M. Effect of Atomically Controlled Interfaces on Fermi-Level Pinning at Metal/Ge Interfaces. *Appl. Phys. Lett.* **2010**, *96*, 162104.
(22) Dash, S. P.; Sharma, S.; Le Breton, J. C.; Peiro, J.; Jaffrès, H.; George, J. M.; Lemaître, A.; Jansen, R. Spin Precession and Inverted Hanle Effect in a Semiconductor near a Finite-Roughness Ferromagnetic Interface. *Phys. Rev. B* **2011**, *84*, 054410.
(23) Tang, J.; Wang, C.-Y.; Hung, M.-H.; Jiang, X.; Chang, L.-T.; He, L.; Liu, P.-H.; Yang, H.-J.; Tuan, H.-Y.; Chen, L.-J.; Wang, K. L. Ferromagnetic Germanide in Ge nanowire Transistors for Spintronics Application. *ACS Nano* **2012**, *6*, 5710−5717.
(24) Tang, J.; Wang, C.-Y.; Jiang, W.; Chang, L.-T.; Fan, Y.; Chan, M.; Wu, C.; Hung, M.-H.; Liu, P.-H.; Yang, H.-J.; Tuan, H.-Y.; Chen, L.-J.; Wang, K. L. Electrical Probing of Magnetic Phase Transition and Domain Wall Motion in Single-Crystalline Mn_5Ge_3 Nanowire. *Nano Lett.* **2012**, *12*, 6372−6379.
(25) Gajdzik, M.; Sürgers, C.; Kelemen, M. T.; Löhneysen, H. v. Strongly Enhanced Curie Temperature in Carbon-Doped Mn_5Ge_3 Films. *J. Magn. Magn. Mater.* **2000**, *221*, 248−254.
(26) Tang, J.; Wang, C.-Y.; Chen, L.-J.; Wang, K. L. *Ge Nanowire Transistors with High-Quality Interfaces by Atomic-Scale Thermal Annealing*, 2012 IEEE 12th Conference on Nanotechnology, Birmingham, U.K., Aug. 20−23, 2012; IEEE: Birmingham, UK, 2012; pp 1−5.
(27) Zhou, Y.; Han, W.; Wang, Y.; Xiu, F.; Zou, J.; Kawakami, R. K.; Wang, K. L. Investigating the Origin of Fermi Level Pinning in Ge Schottky Junctions Using Epitaxially Grown Ultrathin MgO Films. *Appl. Phys. Lett.* **2010**, *96*, 102103.
(28) Panguluri, R. P.; Zeng, C.; Weitering, H. H.; Sullivan, J. M.; Erwin, S. C.; Nadgorny, B. Spin Polarization and Electronic Structure of Ferromagnetic Mn_5Ge_3 Epilayers. *Phys. Status Solidi B* **2005**, *242*, R67−R69.
(29) Picozzi, S.; Continenza, A.; Freeman, A. J. First-Principles Characterization of Ferromagnetic Mn_5Ge_3 for Spintronic Applications. *Phys. Rev. B* **2004**, *70*, 235205.
(30) Iba, S.; Saito, H.; Spiesser, A.; Watanabe, S.; Jansen, R.; Yuasa, S.; Ando, K. Spin Accumulation and Spin Lifetime in p-Type Germanium at Room Temperature. *Appl. Phys. Express* **2012**, *5*, 053004.
(31) Yang, H.-J.; Tuan, H.-Y. High-Yield, High-Throughput Synthesis of Germanium Nanowires by Metal-Organic Chemical Vapor Deposition and Their Functionalization and Applications. *J. Mater. Chem.* **2012**, *22*, 2215−2225.
(32) Tang, J.; Wang, C.-Y; Xiu, F.; Hong, A.; Chen, S.; Wang, M.; Zeng, C.; Yang, H.-J; Tuan, H.-Y; Tsai, C.-J; et al. Single-Crystalline Ni_2Ge/Ge/Ni_2Ge Nanowire Heterostructure Transistors. *Nanotechnology* **2010**, *21*, 505704.
(33) Tang, J.; Wang, C.-Y.; Xiu, F.; Lang, M.; Chu, L.-W.; Tsai, C.-J.; Chueh, Y.-L.; Chen, L.-J.; Wang, K. L. Oxide-Confined Formation of Germanium Nanowire Heterostructures for High-Performance Transistors. *ACS Nano* **2011**, *5*, 6008−6015.
(34) Tang, J.; Wang, C.-Y.; Xiu, F.; Zhou, Y.; Chen, L.-J.; Wang, K. L. Formation and Device Application of Ge Nanowire Heterostructures via Rapid Thermal Annealing. *Adv. Mater. Sci. Eng.* **2011**, *2011*, 316513.
(35) Sze, S. M.; Ng, K. K. *Physics of Semiconductor Devices*; John Wiley & Sons: Hoboken, NJ, 2006.
(36) Furukawa, Y. Electrical Properties of Heavily Doped *n*-Type Germanium. *J. Phys. Soc. Jpn.* **1961**, *16*, 687−694.
(37) Hust, J. G.; Lankford, A. B. *Update of Thermal Conductivity and Electrical Resistivity of Electrolytic Iron, Tungsten, and Stainless Steel*; U.S. Department of Commerce, National Bureau of Standards: Washington, DC, 1984.
(38) Tsymbal, E. Y.; Mryasov, O. N.; LeClair, P. R. Spin-Dependent Tunnelling in Magnetic Tunnel Junctions. *J. Phys.: Condens. Matter* **2003**, *15*, R109−R142.
(39) Chang, L.-T.; Han, W.; Zhou, Y.; Tang, J.; Fischer, I. A.; Oehme, M.; Schulze, J.; Kawakami, R. K.; Wang, K. L. Comparison of Spin Lifetimes in *n*-Ge Characterized between Three-Terminal and Four-Terminal Nonlocal Hanle Measurements. *Semicond. Sci. Technol.* **2012**, *28*, 015018.
(40) Pramanik, S.; Stefanita, C. G.; Patibandla, S.; Bandyopadhyay, S.; Garre, K.; Harth, N.; Cahay, M. Observation of Extremely Long Spin Relaxation Times in an Organic Nanowire Spin Valve. *Nat. Nanotechnol.* **2007**, *2*, 216−219.
(41) Xiong, Z. H.; Wu, D.; Valy Vardeny, Z.; Shi, J. Giant Magnetoresistance in Organic Spin-Valves. *Nature* **2004**, *427*, 821−824.
(42) Sadasiv, G. Galvanomagnetic Effects in Heavily Doped *p*-Type Germanium. *Phys. Rev.* **1964**, *133*, A1207−A1213.
(43) Lin, Y.-C.; Chen, Y.; Shailos, A.; Huang, Y. Detection of Spin Polarized Carrier in Silicon Nanowire with Single Crystal MnSi as Magnetic Contacts. *Nano Lett.* **2010**, *10*, 2281−2287.
(44) Julliere, M. Tunneling between Ferromagnetic Films. *Phys. Lett. A* **1975**, *54*, 225−226.
(45) Sze, S. M.; Irvin, J. C. Resistivity, Mobility and Impurity Levels in GaAs, Ge, and Si at 300 K. *Solid-State Electron.* **1968**, *11*, 599−602.
(46) Sasaki, T.; Oikawa, T.; Suzuki, T.; Shiraishi, M.; Suzuki, Y.; Noguchi, K. Temperature Dependence of Spin Diffusion Length in Silicon by Hanle-Type Spin Precession. *Appl. Phys. Lett.* **2010**, *96*, 122101.
(47) Balandin, A. A. Nanophononics: Phonon Engineering in Nanostructures and Nanodevices. *J. Nanosci. Nanotechnol.* **2005**, *5*, 1015−1022.
(48) Joyce, W. B.; Dixon, R. W. Analytic Approximations for the Fermi Energy of an Ideal Fermi Gas. *Appl. Phys. Lett.* **1977**, *31*, 354−356.
(49) Xiu, F.; Wang, Y.; Kim, J.; Hong, A.; Tang, J.; Jacob, A. P.; Zou, J.; Wang, K. L. Electric-Field-Controlled Ferromagnetism in High-Curie-Temperature $Mn_{0.05}Ge_{0.95}$ Quantum Dots. *Nat. Mater.* **2010**, *9*, 337−344.
(50) Xiu, F.; Wang, Y.; Kim, J.; Upadhyaya, P.; Zhou, Y.; Kou, X.; Han, W.; Kawakami, R. K.; Zou, J.; Wang, K. L. Room-Temperature Electric-Field Controlled Ferromagnetism in $Mn_{0.05}Ge_{0.95}$ Quantum Dots. *ACS Nano* **2010**, *4*, 4948−4954.
(51) Liu, L.; Pai, C.-F.; Li, Y.; Tseng, H. W.; Ralph, D. C.; Buhrman, R. A. Spin-Torque Switching with the Giant Spin Hall Effect of Tantalum. *Science* **2012**, *336*, 555−558.
(52) Behin-Aein, B.; Datta, D.; Salahuddin, S.; Datta, S. Proposal for an All-Spin Logic Device with Built-In Memory. *Nat. Nanotechnol.* **2010**, *5*, 266−270.